Environmental Science & Technology

pubs.acs.org/est

Article

Plutonium Speciation and Oxidation State Distributions in the Presence of Citrate

Matthew B. Comins, Ugras Kaplan, Jeremiah Beam, Adrianne Navarrette, and Amy E. Hixon*

Cite This: *Environ. Sci. Technol.* 2024, 58, 15766−15778

Read Online

ACCESS | Metrics & More | Article Recommendations | Supporting Information

Downloaded via LOS ALAMOS NATL LABORATORY on July 18, 2025 at 17:39:00 (UTC).
See https://pubs.acs.org/sharingguidelines for options on how to legitimately share published articles.

ABSTRACT: We explored the speciation and kinetics of the Pu(VI)-citrate and Pu(III)-citrate systems (pH_m = 2.5−11.0, I = 0.1 M NaCl, T = 23 °C, $O_2(g)$ < 2 ppm) using ultraviolet−visible−near-infrared (UV−vis−NIR) spectrophotometry, solvent extraction, and PHREEQC modeling. Formation constants were determined for $PuO_2(HcitH)(aq)$ ($\log K^\circ_{1,1}$ = 1.09 ± 0.05) and $PuO_2(HcitH)(citH)^{3-}$ ($\log K^\circ_{1,2}$ = −0.20 ± 0.07), and evidence for $(PuO_2)_m(citH_{-k})_n(OH)_x^{2m(3+k)n-x}$ was identified under alkaline conditions. Pu(VI) species were found to be less stable in the presence of citrate than in the absence of citrate ($t \leq$ 168 days); the rate of reduction increased with increasing pH. The direct reduction of Pu(VI) to Pu(IV) was required to fit experimental data in the presence of citrate but did not improve the fit for Pu in the absence of citrate. We also observed increased Pu(III) stability in the presence of citrate ($t \leq$ 293 days), with higher concentrations of Pu(III) favored at lower pH. Finally, we provide evidence of a radiolysis-driven mechanism for the citrate-mediated reduction of plutonium that involves electron transfer from the oxidative breakdown of citrate. Our work highlights the need to investigate the redox effect of organic ligands on plutonium oxidation states under repository-relevant conditions.

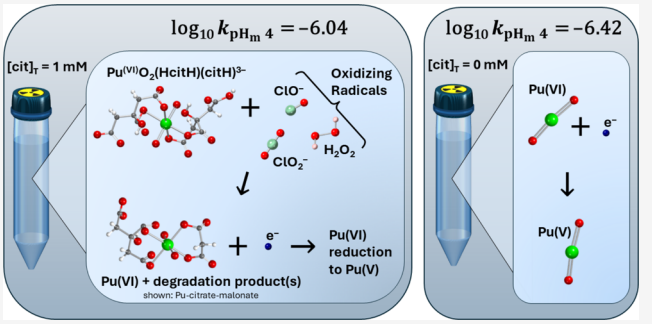

KEYWORDS: *plutonium, citrate, redox reactions, kinetics, WIPP, solvent extraction, UV−vis−NIR, PHREEQC*

1. INTRODUCTION

Understanding plutonium mobility from a geologic repository is necessary for its safe sequestration from humans and the broader environment. The Waste Isolation Pilot Plant (WIPP), located in Carlsbad, New Mexico, is a deep geologic repository for the permanent disposal of defense-related transuranic waste. Recent estimates suggest approximately 3.07 × 10^6 Ci (1.14 × 10^{17} Bq; 10.9 t) of plutonium in WIPP inventory through 2021,[1] but 34 t of surplus plutonium are being actively petitioned for disposal by the National Nuclear Security Administration through their dilute and dispose strategy.[2]

Citrate (cit) is among the group of polycarboxylate ligands and is present throughout the nuclear industry due to its use in decontamination processes. Such ligands are strong chelators because of their multiple functional groups, thus forming strong, stable complexes with plutonium and other actinides (according to the trend An(IV) > An(III) ≈ An(VI) ≫ An(V)).[3] Citrate has four functional groups, three carboxylate and one hydroxyl, of which at most three may be simultaneously bound to a metal due to steric constraints. To distinguish the hydroxyl proton from the carboxylate proton, we adopt a naming scheme where carboxylate protons are written to the left, and the hydroxyl proton is written to the right of "cit". Thus, H_3citH represents the fully protonated ligand and cit^{4-} represents the fully deprotonated ligand.

Though citrate has been shown to undergo chemical,[4] microbial,[5] and radiolytic degradation,[6,7] interactions between plutonium and citrate must still be considered, due to both the excess (>1800 kg)[1] of citrate expected in the WIPP inventory and to the lack of knowledge surrounding citrate stability under WIPP-relevant conditions. A variety of studies regarding Pu-cit (or Pu-analogous) speciation exists, but the exact nature of these complexes remains contested, most commonly with respect to the degree of citrate protonation or plutonium hydrolysis.[5,8−25] Only a small portion of the reported stability constants for Pu-cit complexes are selected for inclusion in the Nuclear Energy Agency's Thermochemical Database (NEA-TDB);[3] the rest present discrepancies or limitations, such as limited pH range or exclusively high ionic strength conditions. Studies concerning Pu-cit complexation under circumneutral to alkaline conditions are especially discrepant (for Pu(IV))[10] or unreported (for Pu(III), Pu(V), and Pu(VI)). Understanding the relevant aqueous Pu-cit species and the

Received: March 20, 2024
Revised: August 12, 2024
Accepted: August 13, 2024
Published: August 20, 2024



ACS Publications

© 2024 American Chemical Society

subsequent effect of citrate on plutonium solubility is needed for equilibrium models used to assess repository safety and performance.

While the effect of citrate on the long-term oxidation state distribution of plutonium is virtually unexplored,[26] other organic ligands, including nitrilotriacetic acid (nta) and ethylenediaminetetraacetic acid (edta), have been shown to stabilize Pu(III) under some conditions.[27,28] Such observations contribute to the overall uncertainty surrounding the equilibrium ratio of Pu(III) to Pu(IV) in the WIPP.[29] Though Pu(VI) or Pu(V) species are not expected to contribute to long-term repository performance due to anoxic conditions and excess of reducing iron species, understanding the behavior of higher-valent plutonium in the presence of organic ligands is necessary for early repository and environmental settings (e.g., in the event of a repository breach) where Pu may not yet be in its reduced form or where oxidizing radiolysis species may exist.[29] Higher-valent plutonium behavior in the presence of organic ligands may also have relevance to separations and the nuclear fuel cycle (e.g., PUREX), where advances and optimizations are still sought.[30,31] Thus, determining both the thermodynamically stable Pu oxidation state(s) and the evolution of Pu oxidation state distributions in the presence of citrate is required for accurate predictive modeling of plutonium mobility in WIPP and other repository environments. Though a high ionic strength is WIPP-relevant, our approach involved low-ionic-strength systems (0.1 M) to obtain a fundamental understanding of the effect of citrate on Pu behavior. WIPP-relevant ionic strengths (5.3−7.4 M)[32] would necessitate the need for Pitzer parameters for accurate modeling and extrapolation to I = 0, which are lacking for the Pu-cit system.

2. MATERIALS AND METHODS

2.1. Plutonium Working Solution Preparation. A ^{242}Pu stock solution (originally plutonium oxide purchased from Oak Ridge National Laboratory) with an isotopic distribution of 0.003% ^{238}Pu, 0.005% ^{239}Pu, 0.022% ^{240}Pu, 0.006% ^{241}Pu, 99.962% ^{242}Pu, and 0.002% ^{244}Pu was used for samples in Figure 1a (conducted at LANL-Carlsbad). A Pu(VI) working solution was prepared by evaporating an aliquot of the stock solution to near-dryness, diluting with 0.5 mL of concentrated HCl(aq) (TraceMetal grade, Fisher), heating to dryness, and fuming with concentrated $HClO_4$(aq) (TraceMetal grade, Fisher). After fuming, the heat was turned down to limit fuming and facilitate evaporation, after which the stock was diluted with 1 mL of Milli-Q water and analyzed with ultraviolet−visible−near-infrared (UV−vis−NIR) spectroscopy. No peaks other than those associated with Pu(VI) were observed for a sample with $[Pu]_T \approx 0.3$ mM.

For all other samples, a ^{239}Pu stock solution from Pacific Northwest National Laboratory was used with an isotopic distribution of 0.008% ^{238}Pu, 93.629% ^{239}Pu, 6.304% ^{240}Pu, 0.041% ^{241}Pu, and 0.019% ^{242}Pu. A Pu(VI) working solution was prepared by evaporating an aliquot of the stock solution to dryness, adding 250 μL of concentrated HNO_3(aq) (68−70%, VWR) and 50 μL of concentrated $HClO_4$(aq) (69−72%, VWR), and leaving overnight for oxidation at 120 °C. The solution was then heated to complete dryness and redissolved in 110 μL of ultrapure water. Oxidation state confirmation was obtained from UV−vis−NIR spectrophotometry or solvent extraction-based oxidation state analysis. The typical yield was ≥90−95% Pu(VI). A Pu(III) working solution was prepared by evaporating an aliquot of the stock solution to dryness, adding 4 mL of concentrated HBr (47−49%, VWR), and heating to dryness again. Successive small additions of HBr (e.g., 500 μL) and reheating to dryness were sometimes necessary until a deep blue color was achieved, after which the stock was diluted with 0.3 M HCl and transferred into the glovebox. A small aliquot was used for analysis by UV−vis−NIR spectroscopy or solvent extraction-based oxidation state analysis, with typical yields of 90−99% Pu(III).

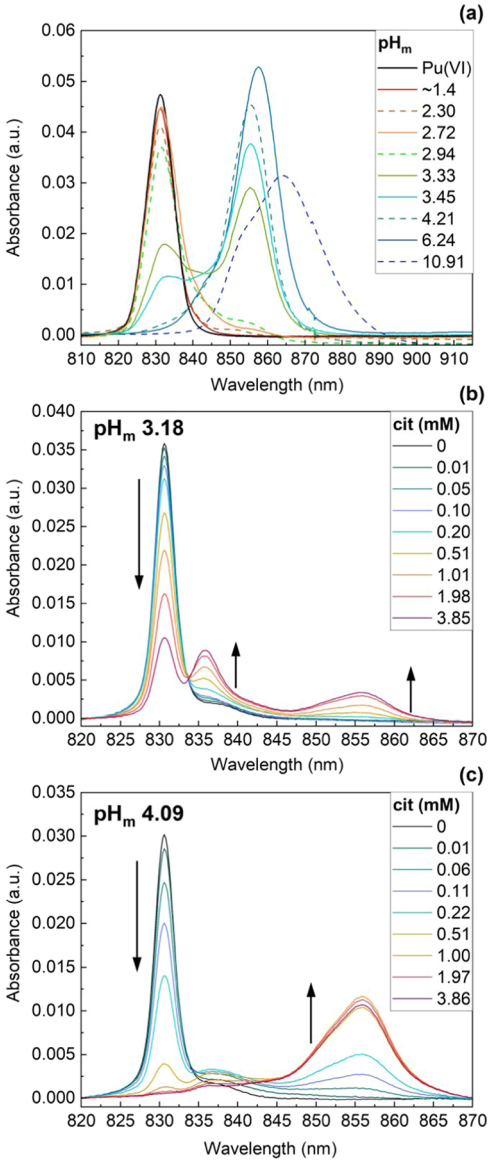

Figure 1. UV−vis−NIR absorption spectra of (a) Pu(VI) and citrate as a function of pH under oxic (solid lines) and anoxic (dashed lines) conditions, normalized to $[Pu]_T$ = 0.3 mM, with $[cit]_T$ = 1.00 ± 0.01 mM, and Pu(VI) in dilute $HClO_4$ (black solid line); (b) Pu(VI) at pH_m 3.18 as a function of citrate concentration ($[Pu(VI)]_T$ = 0.071 ± 0.001 mM, $[cit]_T$ = 0−3.85 ± 0.02 mM); (c) Pu(VI) at pH_m 4.09 as a function of citrate concentration ($[Pu(VI)]_T$ = 0.060 ± 0.001 mM, $[cit]_T$ = 0−3.86 ± 0.30 mM). Scans from (b) and (c) were conducted in air and normalized to account for dilution by the addition of citrate stock solution. Spectra were acquired within 2 h of sample preparation.

2.2. Batch Experiments. Batch reactors were prepared and stored in an N_2(g)-circulating MBraun glovebox (O_2(g) < 2 ppm, T = 23 ± 2 °C) using Milli-Q water that was boiled for

https://doi.org/10.1021/acs.est.4c02803
Environ. Sci. Technol. 2024, 58, 15766−15778

1 h while being purged with $N_2(g)$. The water was subsequently placed on a stirrer in the glovebox with the cap loose to allow for equilibration with the inert atmosphere. No dissolved oxygen was observable with a rhodazine D test kit (detection limit of 2 ppb). Between samplings, reactors were sealed with Parafilm and placed in double containment.

Citrate stock solutions were prepared from $NaH_2citH(s)$ (99%, Sigma-Aldrich) or $Na_3citH{\cdot}2H_2O(s)$ (≥99%, RPI Research Products). Ionic strength was kept constant at 0.1 M with NaCl (≥99%, Fisher). Adjustments to pH were made by adding 0.1 M HCl or NaOH. An Agilent 7900 quadrupole inductively coupled plasma-mass spectrometer was used for the determination of total plutonium concentration in Figure 1a and was calibrated with an external ^{242}Pu standard (Eckert and Ziegler) and indium internal standard (1000 ppm in 2% HNO_3, High Purity Standards). Liquid scintillation counting was used for determining the aqueous plutonium concentrations in all other experiments. Amicon 10 kDa (or, for one sampling of the Pu(III)-cit system, 3 kDa) centrifugal filters were used to remove the colloidal/precipitated Pu fraction from sampled batch reactors prior to solvent extraction at 14,000 rpm for 10 min.

Batch reactors for long-term anoxic kinetic studies were prepared using amber vials, including separate reactors for Pu-cit and Pu controls at $[cit]_T$ = 1 mM, [Pu] = 0.09−0.11 mM, and pH_m = 2.5−11, with the control corresponding to Pu without citrate. The sampling period for the Pu(VI) system ranged from 0 to 168 and 0 to 144 days for the Pu-cit and Pu(VI) controls, respectively. The oxidation of Pu(III) to Pu(IV) occurred comparatively slower, requiring sampling points of up to 293 and 282 days for the Pu-cit and Pu(III) controls, respectively. Each sampling involved the measurement of pH and E_h (see the Supporting Information (SI)), UV−vis−NIR spectrophotometry, and oxidation state analysis.

2.3. UV−Vis−NIR Spectrophotometry. Spectrophotometric measurements were performed using a Varian Cary 5000 or 6000i instrument at 23 ± 2 °C to determine Pu-cit speciation. Quartz cuvettes (path length of 1 cm) were sealed with Parafilm prior to measurement. Samples from most batch reactors were measured anoxically with a Harrick FiberMate fiber optic accessory connected to the glovebox. A spectral bandwidth (SBW) of 0.6 nm was used on the Varian Cary 5000 (scan rate = 60 nm min^{-1}). For measurements using the Cary 6000i, an SBW of 1 nm was used for anoxic measurements (scan rate = 24 nm min^{-1}) and an SBW of 2 (scan rate = 60 nm min^{-1}) was used for oxic measurements (pH_m < 4.1). Samples were not filtered prior to each scan, enabling detection of Pu(IV) colloids (if present above the detection limit of ∼10 μM) through a scattering profile, characteristic peak at 614 nm, or a broad peak from ∼790 to 850 nm.[33,34] Calibrations were regularly performed using the Agilent-recommended tests in the Cary Validation software to ensure spectral validity. Peak fitting was performed through the Peak Analyzer function in OriginPro using a Gaussian fitting function with a convergence requirement of $\chi^2 \leq 10^{-6}$.

2.4. Oxidation State Analysis. Solvent extraction was utilized to determine the distribution of the Pu oxidation states after filtration. This included 0.5 M bis(2-ethylhexyl)-phosphoric acid (HDEHP) dissolved in hexane and 0.025 M 4-benzoyl-3-methyl-1-phenyl-2-pyrazolin-5-one (PMBP), also dissolved in hexane, as extractants, where HDEHP extracts Pu(IV)/Pu(VI) into the organic phase, and PMBP extracts Pu(IV) into the organic phase.[35−37] A separate extraction using dichromate and PMBP was used, which oxidizes Pu(III) to Pu(IV), thus enabling quantification of aqueous Pu(III) when compared to measurements in the absence of dichromate.[36,38,39] The validity of this solvent extraction approach is described in SI. Coprecipitation using LaF_3 is known to effectively precipitate Pu(III) and Pu(IV), leaving the Pu(V/VI) pair in the aqueous phase,[40,41] and was used to substantiate the ratio of Pu(III)/Pu(IV) to Pu(V)/Pu(VI) determined by solvent extraction (pH = −0.2). Solvent extraction results were in good agreement with those of coprecipitation, rarely exceeding a difference of 2% between techniques, and are, therefore, not presented here. The difference in the amount of plutonium removed by filtration prior to solvent extraction ($[Pu]_{T,\ initial} - [Pu]_{T,\ filtrate}$) was assumed to be a solid or colloidal phase.

Following the desired reaction time, a 0.5 mL aliquot of the sample was diluted with 4.5 mL of 0.3 M HCl. A 0.5 mL aliquot was analyzed by liquid scintillation counting (LSC) to determine the total aqueous phase concentration of plutonium, and the remainder was filtered and used for the solvent extraction and coprecipitation procedures. Aliquots of each aqueous or organic phase were mixed with 5 mL of OptiPhase HiSafe 3 scintillation cocktail (PerkinElmer) and analyzed by a PerkinElmer Tri-Carb 3100 TR liquid scintillation counter. Uncertainties for the concentration of each oxidation state were obtained by propagating the counting error from LSC measurements, the distribution coefficients for Pu(VI) in HEDHP[42] and Pu(IV) in PMBP,[43] and the difference between total measured Pu activity in each separation (aqueous + organic phases) and the calculated Pu activity in the diluted sample (which is used to calculate absolute concentration for each oxidation state).

3. RESULTS AND DISCUSSION

3.1. Pu(VI) Speciation in the Presence of Citrate. *3.1.1. Pu(VI) Spectrophotometry (Oxic and Anoxic).* Oxic and anoxic spectra were collected as a function of pH_m to probe changes in the speciation (Figure 1a). Evidence for Pu(VI)-cit complexation was seen as low as pH_m 2.30, as demonstrated by a decrease in intensity of the Pu(VI) aquo ion peak at 831 nm and the growth of a peak at 836 nm, which is less visible under the conditions of spectra acquisition in Figure 1a (SBW = 0.6 nm) but is clearly observed in Figure 1b (SBW = 2 nm). Upon increasing pH_m, the peaks at 831 and 836 nm were replaced by a single peak at 856 nm that was the predominant peak at pH_m ≥ 3.33 (Figure 1a). Above pH_m 6, where Pu(VI) hydrolysis species are predominant,[44,45] the 856 nm peak was slightly red-shifted and replaced by a peak at 865 nm that became predominant at pH_m 10.91. As citrate deprotonates, complexation with Pu(VI) increases. Upon increasing the concentration of citrate at pH_m 3.18, peaks at 836 and 856 nm replaced the 831 nm PuO_2^{2+} peak (Figure 1b); at pH_m 4.09, only the 856 nm peak grew with increasing citrate concentration (Figure 1c). Nebel and Anders[11] assigned 1:1 and 1:2 species to the peaks at 836 and 856 nm, respectively.

Identification of Pu(VI)-cit species under neutral to alkaline conditions is challenging due to the presence of Pu(VI) hydrolysis peaks. The monomeric $PuO_2(OH)_2(aq)$ species is expected at 850−851 nm[46,47] and the $PuO_2(OH)_3^-$ species is expected at 862−864 nm.[44,47] Deconvolution of spectra at pH_m 8.23 and 10.94 using a fixed peak at 863 nm revealed a peak at 874 nm (Figure S1), suggesting a Pu-cit or ternary Pu-cit−OH complex of unknown stoichiometry (i.e.,

https://doi.org/10.1021/acs.est.4c02803
Environ. Sci. Technol. 2024, 58, 15766−15778

$(PuO_2)_m(citH_{-k})_n(OH)_x^{2m-(3+k)n-x}$, with m number of plutonyl ions, n number of citrate moieties, x number of hydroxyl groups, and k hydroxyl group protons). Attempts to fit the same peaks (i.e., 851, 863, and 874 nm) using a Gaussian function in the pH_m 10.91 spectrum without citrate did not converge, further validating the 874 nm peak. Assigning the 874 nm peak to $(PuO_2)_2(citH)_2(OH)_2^{4-}$ or $(PuO_2)_3(O)(citH)_3^{8-}$ (by analogy with the U(VI) complexes identified by Kretzschmar et al.[48]) did not produce equilibrium modeling results that reasonably matched our spectral observations and likely speaks to the known differences in U(VI) and Pu(VI) speciation.[44] Further work is needed to constrain the stoichiometry and formation constant of this new Pu(VI)-cit complex, for example, through studies that explore variable citrate concentrations under alkaline conditions using advanced spectroscopic techniques (e.g., X-ray absorption spectroscopy) and computational modeling.

3.1.2. Comparison to Pu(VI) Thermodynamic Models. To perform speciation calculations, we assumed that the 1:1 complex formed according to reaction 1

$$PuO_2^{2+} + H_2citH^- \rightleftharpoons PuO_2(HcitH)(aq) + H^+ \quad (1)$$

because of the pK_a values for citrate (Figure 2a) and the pH_m range ($pH_m \approx 2.5-3.5$) where we observed the 836 nm peak. Likewise, we assumed that the 1:2 complex was formed according to reaction 2.

$$PuO_2(HcitH)(aq) + HcitH^{2-} \rightleftharpoons PuO_2(HcitH)(citH)^{3-} + H^+ \quad (2)$$

The formation constants for the 1:1 and 1:2 complexes were $\log K^\circ_{1,1} = 1.09 \pm 0.05$ and $\log K^\circ_{1,2} = -0.20 \pm 0.07$, respectively. Assuming the formation of fully deprotonated complexes resulted in equilibrium models that vastly overestimated the predominance of the 1:2 complex. It is not clear from the spectroscopy when $PuO_2(HcitH)(citH)^{3-}$ deprotonates, though it might be correlated to a ~2 nm red-shift of the 856 nm peak that occurs between pH_m 3.98 and 6.24. These peaks are too close together to be used in calculating the log K for this reaction.

While the hydroxyl group of free citrate only deprotonates at a very high pH ($pK_a = 14.4 \pm 0.3$),[49] it may coordinate metals over a much broader pH range.[3,21,48,50−58] This is especially plausible for actinyl ions, where citrate coordination is limited to the equatorial plane and, due to steric constraints, only two carboxyl groups may coordinate to an actinyl ion.[3] It is for this reason that Hummel et al.[3] suggest that the stability of UO_2citH^- is similar to that of $UO_2(HcitH)(aq)$. Such steric constraints also substantiate the singly protonated 1:1 and 1:2 Pu(VI)-cit complexes identified in this study. In the case of $PuO_2(HcitH)(aq)$, the coordination mode described by Hummel et al.[3] should result in at least one protonated, uncoordinated carboxyl group (Figure 3), given the predominance of $H_3citH(aq)$ and H_2citH^- within the pH range where this complex is stable. The two structures proposed in Figure 3a,b are chemically equivalent (i.e., same degree of citrate protonation) but panel (b) indicates hydroxyl coordination and deprotonation. Likewise, the $PuO_2(HcitH)(citH)^{3-}$ complex shown in Figure 3c, with bidentate coordination from two carboxylate groups, would be chemically identical with a complex with hydroxyl coordination from either citrate molecule, as long as there was proton transfer from the hydroxyl to a free carboxylate group. Understanding the extent

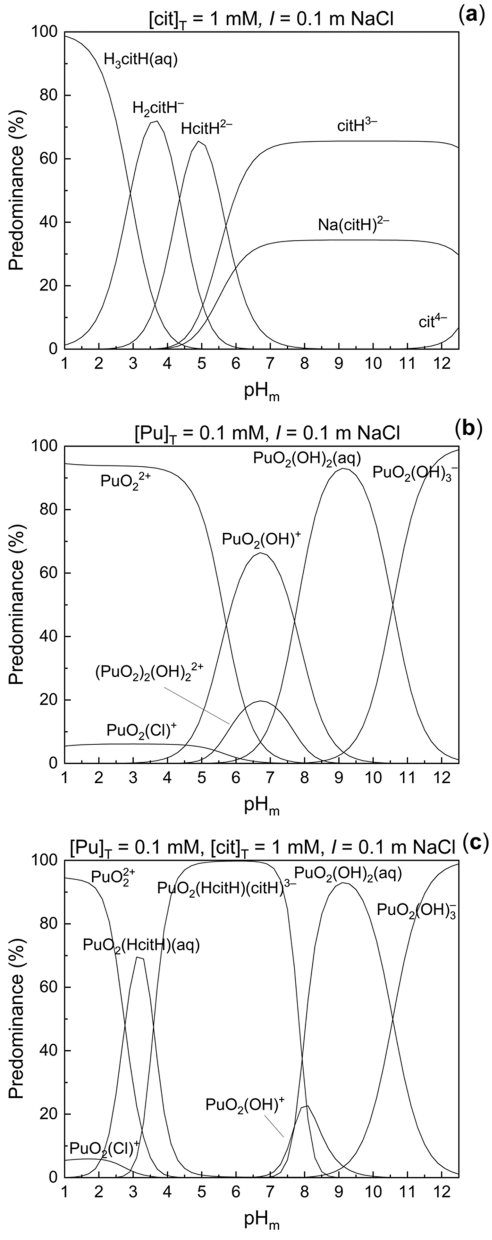

Figure 2. Predominance diagrams created using PHREEQC of (a) 1 mM citrate, (b) 0.1 mM Pu(VI), and (c) 0.1 mM Pu(VI) and 1 mM citrate with values for Pu-cit complexes determined in this work. Formation constants are reported in Table S4. Precipitation was not considered.

of hydroxyl involvement from citrate at pH < 4 (i.e., most feasibly for the 1:1 complex) would aid in the future identification and inform the stoichiometry of ternary hydrolyzed Pu(VI)-cit complexes, notably the $(PuO_2)_m(citH_{-k})_n(OH)_x^{2m-(3+k)n-x}$ complex described above, whereby x number of coordinated OH^- groups could be assigned.

3.2. Pu(VI) Reduction in the Presence of Citrate. *3.2.1. Pu(VI) Spectrophotometry (Anoxic).* The rate of reduction of Pu(VI) to Pu(V) and Pu(IV) was correlated with the degree of citrate complexation. Speciation calculations (Figure 2c) suggest that $Pu^{VI}O_2^{2+}$ is the dominant species (68.9%) and $Pu^{VI}O_2(HcitH)(aq)$ represents 26.5% of the total species at pH_m 2.50. The slight bathochromic shift of the Pu(VI) aquo ion observed at pH_m 2.49 (Figure 4a) indicates

https://doi.org/10.1021/acs.est.4c02803
Environ. Sci. Technol. 2024, 58, 15766−15778

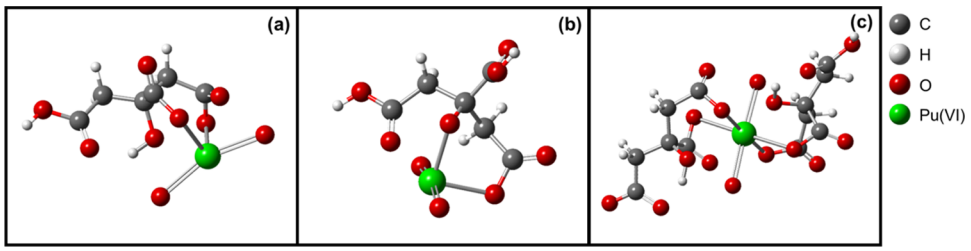

Figure 3. Proposed molecular structures (made using CrystalMaker X) of possible coordination modes for $PuO_2(HcitH)(aq)/PuO_2(H_2cit)(aq)$ (a, b) and $PuO_2(HcitH)(citH)^{3-}$ (c), including bidentate coordination with two carboxyls (a), bidentate coordination with a carboxyl and the hydroxyl (b), and bidentate coordination through the carboxyl groups of two citrate molecules (c).

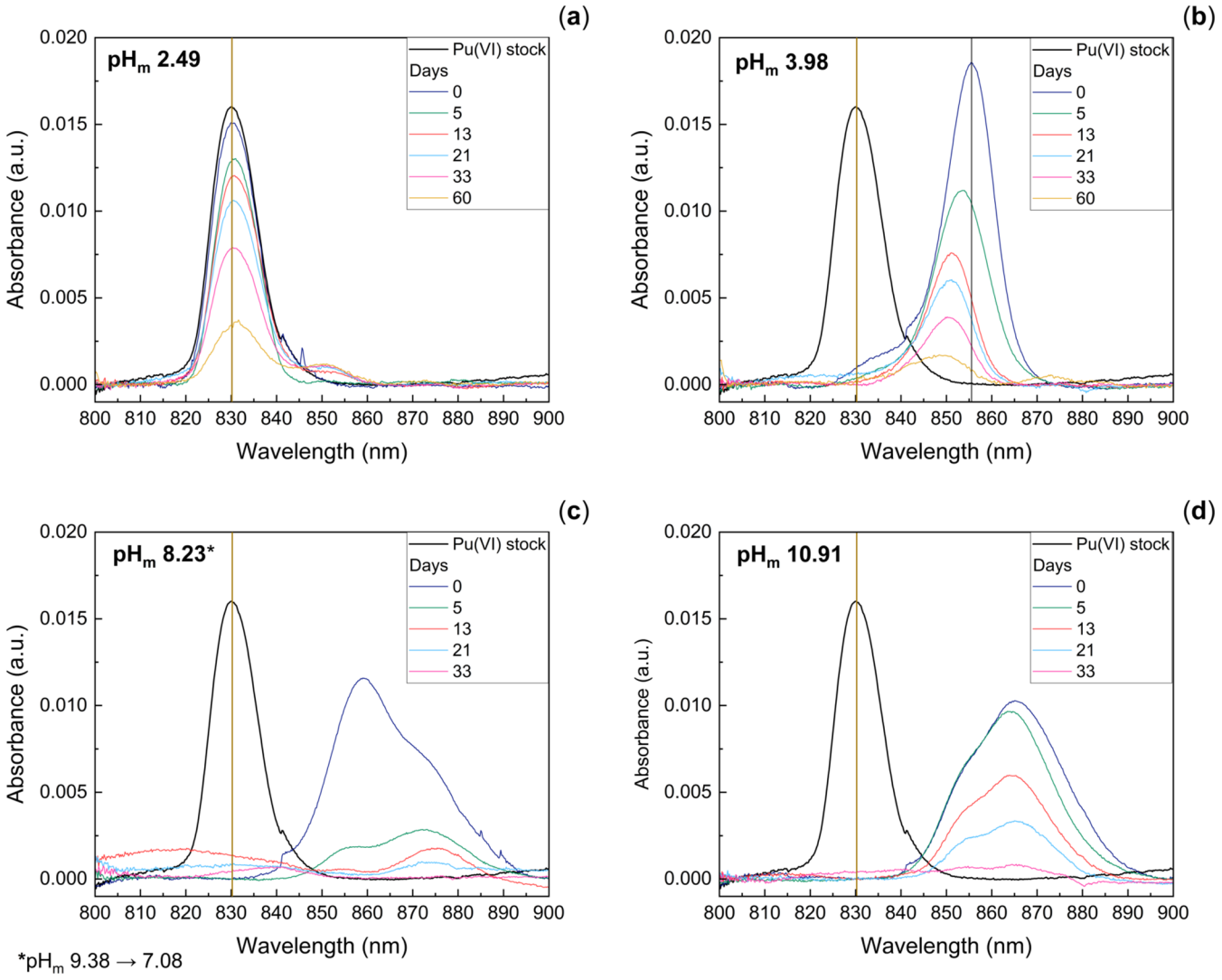

Figure 4. UV−vis−NIR absorption spectra of anoxic Pu(VI)-citrate reactors as a function of time and pH_m. $[Pu]_T = 0.113 \pm 0.001$ mM, $[cit]_T = 1.00 \pm 0.02$, and ionic strength was kept constant at 0.1 M with NaCl. The decrease in pH for the pH_m 8.23 sample is attributed to Pu hydrolysis and precipitation.

citrate complexation and supports these speciation calculations. Experimental spectrophotometric observations of Pu(VI) reduction in the presence of citrate indicate a faster rate of Pu(VI) reduction at pH_m 3.98 than at pH_m 2.49, where the 1:2 Pu(VI)-cit complex is expected to be predominant (Figure 4b). Note that the 856 nm peak (characteristic of the 1:2 complex) exhibits a blue shift over time toward 851 nm (Figure 4b). Speciation was likely mixed in the pH_m 8.23 reactor (Figure 4c), where the spectrum was interpreted as having an approximately equal distribution of $Pu^{VI}O_2(citH)_2^{4-}$ (856 nm) and $(Pu^{VI}O_2)_m(citH_{-k})_n(OH)_x^{2m-(3+k)n-x}$ (874 nm) at time zero (see Figure S1). At pH_m 10.91, a mixture of Pu(VI) hydrolysis species and Pu(VI)-cit complexes was observed (Figure 4d), based on deconvoluted peaks at 852, 863, and 874 nm (Figure S1). The rate of reduction at pH_m 10.91 could be slower than that of pH_m 8.23 due to the hydrolysis of Pu(VI).[59]

https://doi.org/10.1021/acs.est.4c02803
Environ. Sci. Technol. 2024, 58, 15766−15778

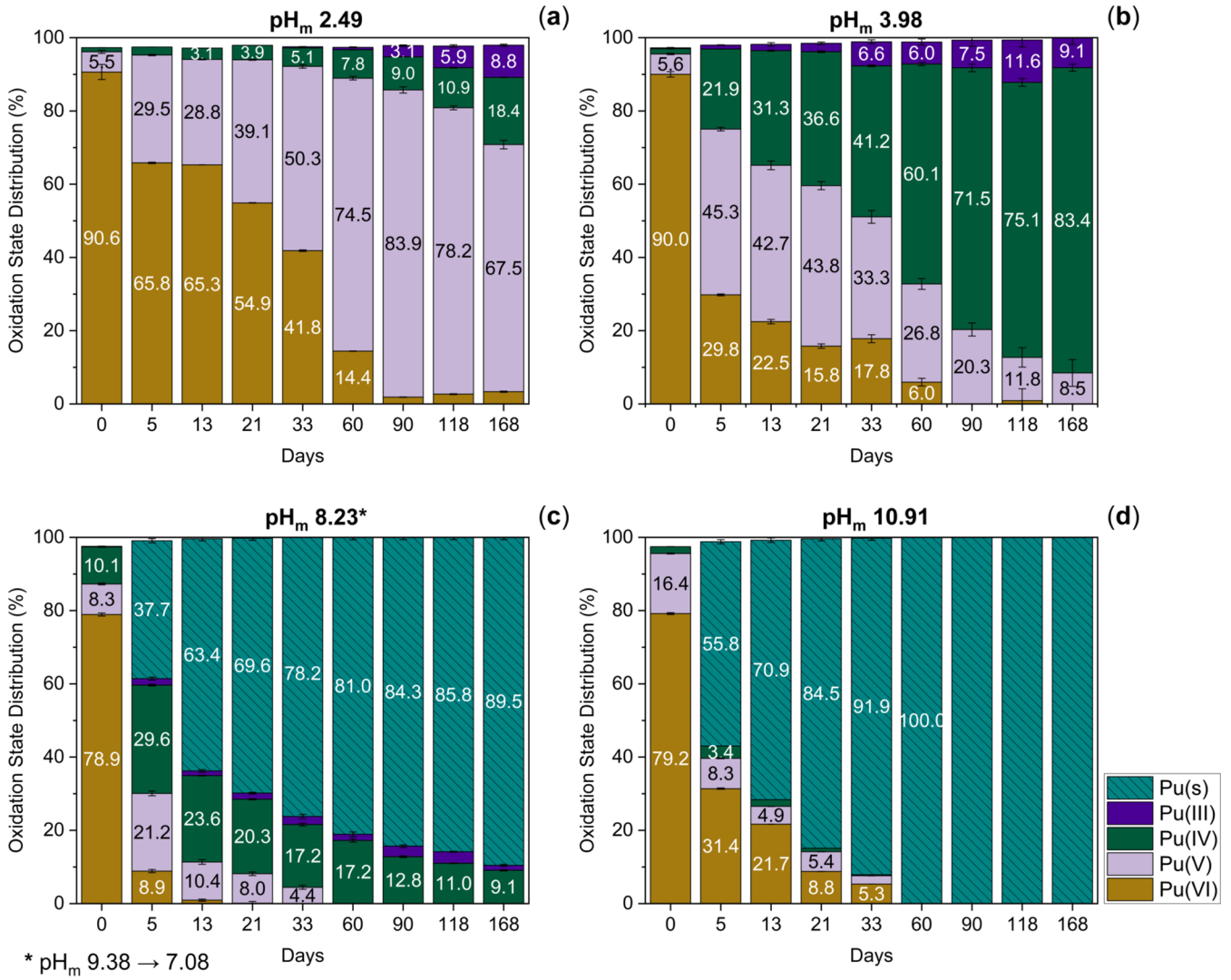

Figure 5. Oxidation state distributions for the Pu(VI)-citrate system. Experimental conditions: $[Pu]_T$ = 0.113 ± 0.001 mM, $[cit]_T$ = 1.00 ± 0.02 mM, and I = 0.1 M NaCl. Pu(s) is used to account for precipitated Pu of any oxidation state.

3.2.2. Oxidation State Analysis of the Pu(VI) System. Oxidation state analysis (Figure 5) supports the observed relative rates of Pu(VI) and Pu(V) reduction in the presence of citrate. The predominant oxidation state in the pH_m 2.49 reactor was Pu(V) after about 30 days, and the rate of Pu(VI) reduction to Pu(V) was faster than that of Pu(V) reduction to Pu(IV), presumably due to the required breaking of *-yl* oxygen bonds. Reduction of Pu(VI) to Pu(V) and Pu(V) to Pu(IV) was faster at pH_m 3.98 than at pH_m 2.49, with Pu(V) to Pu(IV) reduction still being slower than Pu(VI) to Pu(V) at this pH. This observation supports the possibility of citrate-mediated reduction of plutonium, given the greater degree of Pu(VI)-cit complexation at pH_m 3.98.

Aqueous plutonium concentrations decreased with time in the pH_m 8.23 and 10.91 reactors, suggesting that precipitation had occurred, despite the presence of excess citrate. The same phenomenon was observed for Pu(VI) controls with $pH_m \geq$ 7.41 as plutonium was reduced to Pu(IV) (Figure S3). In the presence of citrate, some aqueous Pu(IV) remained in the pH_m 8.23 reactor throughout the sampling period, while virtually no detectable aqueous plutonium remained in the filtrate from the pH_m 10.91 reactor after 33 days. Removal of aqueous Pu(VI) at pH_m 8.23 was comparatively rapid (89 and 99% reduced after 5 and 13 days, respectively) compared to pH_m 10.91 (60 and 73% reduced after 5 and 13 days), which suggests that Pu(VI) hydrolysis might inhibit Pu(VI) reduction in the presence of citrate.

These observations highlight the importance of speciation when considering redox potentials. For example, Hixon and Powell[60] propose that Pu(V) reduction at mineral surfaces is driven by the Nernstian favorability of Pu(IV) surface complexes or Pu(IV) precipitates. The authors describe how the Gibb's free energy would be low enough to promote the reduction of Pu(V) to Pu(IV), which is supported by surface complexation constants that are 9 orders of magnitude higher for Pu(IV) than Pu(V). The same concept can be applied to the present work, where we observe an inhibitory effect of Pu(VI) hydrolysis on Pu(VI) reduction in the presence of citrate at pH_m 10.9, indicating that higher-order Pu(VI) hydrolysis products (e.g., $PuO_2(OH)_3^-$) are more stable than Pu(VI)-cit complexes. Likewise, precipitation of Pu was observed under alkaline conditions, regardless of whether citrate was present. While the solid phase in equilibrium with these reactors was not directly analyzed, it is believed to be a Pu(IV) material, given that the observed pe values were within the stability field of Pu(IV) (Figure S2) and the known

https://doi.org/10.1021/acs.est.4c02803
Environ. Sci. Technol. 2024, 58, 15766−15778

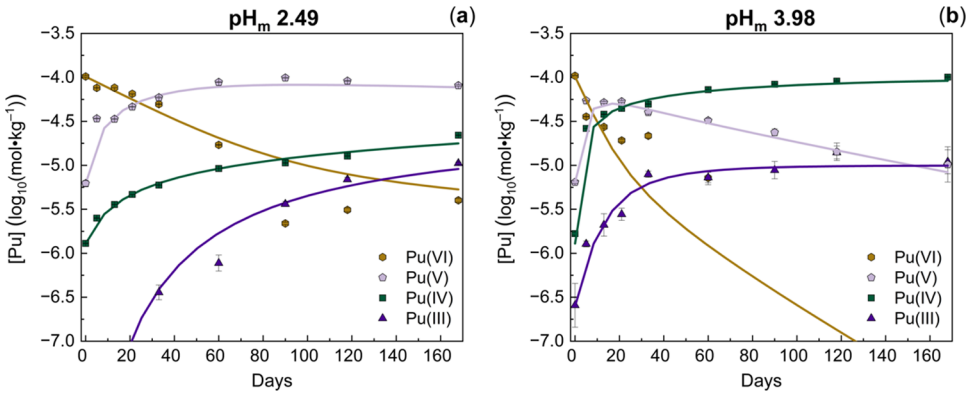

Figure 6. Kinetic models created with PHREEQC of Pu(VI)-citrate system at (a) pH$_m$ 2.49 and (b) pH$_m$ 3.98. Solid lines are model curves with a corresponding color for each Pu oxidation state. Reactions and rate constants are listed in Table 1. $[Pu]_T$ = 0.113 ± 0.001 mM, $[cit]_T$ = 1.00 ± 0.02 mM, I = 0.1 M NaCl.

Table 1. List of Reactions and Rate Constants Used in the Kinetic Models for the Pu(VI)-Citrate System[a]

	rate constant (log$_{10}$), k		
reaction	pH$_m$ 2.49	pH$_m$ 3.98	k units
Pu(VI) → Pu(V)	−6.51	−6.04	s^{-1}
Pu(VI) → Pu(IV)	−7.68	−6.28	s^{-1}
Pu(V) → Pu(IV)	−7.74	−6.89	s^{-1}
3Pu(V) + 4H$^+$ → Pu(III) + 2Pu(VI) + 2H$_2$O	0.18	1.32	M^{-6} s^{-1}
3Pu(IV) + 2H$_2$O → 2Pu(III) + Pu(IV) + 4H$^+$	0.10	0.10	M^{-4} s^{-1}

[a]Uncertainty for rate constants is ±0.01 log$_{10}$ units (2σ).

Table 2. List of Reactions and Rate Constants Used in Kinetic Models for the Pu(VI) System in the Absence of Citrate[a]

	rate constant (log$_{10}$), k		
reaction	pH$_m$ 2.54	pH$_m$ 3.86	k units
Pu(VI) → Pu(V)	−6.60	−6.42	s^{-1}
3Pu(V) + 4H$^+$ → Pu(III) + 2Pu(VI) + 2H$_2$O	0.18	0.18	M^{-6} s^{-1}
3Pu(IV) + 2H$_2$O → 2Pu(III) + Pu(VI) + 4H$^+$	0.10	0.10	M^{-4} s^{-1}

[a]Uncertainty for rate constants is ±0.01 log$_{10}$ units (2σ).

thermodynamic favorability of Pu(IV) hydrolysis products.[61] A greater thermodynamic stability can therefore be attributed to Pu(OH)$_4$(aq) and Pu(IV) solid phases compared to Pu(IV)-cit species above pH$_m$ 8.

Aqueous Pu(III) was observed in reactors up to pH ≤ 8.23. While such concentrations of Pu(III) may result from Pu(IV) and Pu(V) disproportionation, Pu(III) stabilization by organic ligands has been previously observed,[27,28] highlighting the potential need to include such effects in repository performance assessments.

3.2.3. Pu(VI) Kinetic Modeling. Reaction rates for plutonium reduction in the presence of citrate were treated as pseudo-first-order reactions given the apparent effect of citrate on Pu reduction and the excess of citrate used in this system. The concentration of a given plutonium oxidation state at time, t, was calculated using the example in eq 3

$$\frac{d[Pu(V)]}{dt} = k'[Pu(VI)] \quad (3)$$

where k' is the pseudo-first-order rate constant for Pu(VI) reduction in the presence of citrate. At both pH$_m$ 2.49 and 3.98, $\frac{d[Pu(IV)]}{dt}$ was best described as being generated from reduction of Pu(V) and direct reduction of Pu(VI) to Pu(IV) (see Figure S4 for model comparison without this reaction). This latter reaction was not needed to describe Pu(VI) reduction in the absence of citrate (Figure S5), suggesting that the direct reduction of Pu(VI) to Pu(IV) is a citrate-mediated process. Both Pu(IV) and Pu(V) disproportionations were included in the models in Figure 6.

The rate of Pu(V) disproportionation (Table 1) is slower in this work than observed in Connick (log$_{10}$ k = 2.32).[62] This may be primarily due to the fourth-order dependence of the hydrogen ion concentration for this reaction, where Connick[62] observed disproportionation in 0.5 M HCl. The faster rate of Pu(V) disproportionation at pH$_m$ 3.98 compared to pH$_m$ 2.49, however, may be explained by a greater degree of citrate complexation at pH$_m$ 3.98, where Pu(V) becomes less stable toward the apparent reducing capacity of citrate toward plutonium. Little is known about Pu(V) stability in the presence of citrate, so more work is needed in this respect. For Pu(IV) disproportionation, the same rate described in Connick[62] was found suitable for use in both the pH$_m$ 2.49 and 3.98 models.

Kinetic modeling of higher-pH reactors presents difficulties without having characterized the solid phase throughout the duration of the experiment. However, a comparison of rate constants at lower pH values shows that Pu(VI) reduction is

https://doi.org/10.1021/acs.est.4c02803
Environ. Sci. Technol. 2024, 58, 15766−15778

quantitatively slower in the absence of citrate (Table 2). Under neutral to alkaline conditions, the rates of Pu(VI) reduction in the absence of citrate are qualitatively far slower (Figure S3c–e) than in the presence of excess citrate (Figure 5c,d).

Because it was treated as a pseudo-first-order reaction, the reaction order of Pu(V/VI) reduction with respect to citrate, β, was assumed to be zero in both pH_m 2.49 and 3.98 models, and the rate constant in the presence of excess citrate, k', was adjusted accordingly to model empirical data. In the future, measurements of $[cit]_T$ could be made at various times during the sampling period to determine β using the integral method, as in $\left(\frac{1}{[cit]_0\cdot[Pu(VI)]_0}\right)\ln\left(\frac{([Pu(VI)]_0\cdot[cit])}{([cit]_0\cdot[Pu(VI)])}\right) = kt$ for Pu(VI) + cit → Pu(V) (where subscript "0" denotes a reactant's initial concentration), or the initial concentration of citrate could be varied, eliminating the need to measure $\frac{d([cit])}{dt}$.[63]

3.3. Pu(III) and Pu(IV) Speciation in the Presence of Citrate. Pu(III)-citrate speciation has been virtually unexplored,[14] but numerous studies are available with Ln(III) or An(III) analogs.[12,18−21,23,25,54,55,64−67] Under acidic to circumneutral conditions, the NEA-TDB selects stability constants for $Am(HcitH)^+$, $Am(citH)(aq)$, $Am(HcitH)_2^-$, and $Am(citH)_2^{3-}$, but none for Pu(III)-citrate complexes.[3] Evidence for citrate complexation at pH_m 2.92 was seen spectroscopically by exaltation of the 601 nm Pu(III) aquo ion peak (Figure 7). Upon increasing the pH_m, the 601 nm peak redshifted to 608 nm.

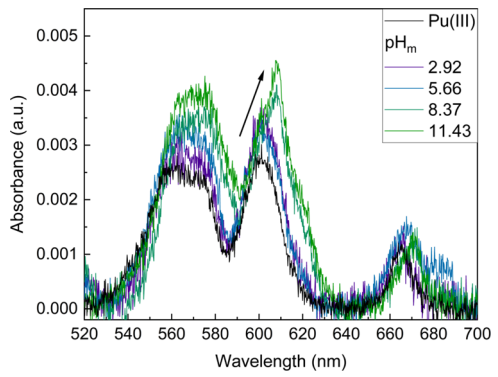

Figure 7. UV−vis−NIR absorption spectra of the initial samplings of the Pu(III)-citrate system. Spectra are normalized to [Pu(III)] = 0.085 mM. The black spectrum indicates Pu(III) in 0.3 M HCl in the absence of citrate. Experimental conditions: $[Pu]_T$ = 0.093 ± 0.001 mM, $[cit]_T$ = 1.00 ± 0.02 mM, and I = 0.1 M NaCl. Spectra were acquired within 2 h of sample preparation.

Spectroscopic evidence for Pu(IV)-citrate species appears after 14 days except at pH_m 11.4, where Pu(IV) hydrolysis (and subsequent precipitation) occurs (Figure S6). The observed Pu(IV)-citrate peaks at 446, 498, and 690 nm do not change with increasing pH, suggesting that the speciation does not change with pH. This most likely corresponds to a 1:2 Pu(IV)-cit complex, which is expected to be predominant under the conditions of this study.[8,9,22] Though Pu(IV) has been found to form a hexamer in solution with ligands including 1,4,7,10-tetraazacyclododecane-1,4,7,10-tetraacetic acid (DOTA) and acetate,[68,69] we found no conclusive evidence through X-ray scattering or X-ray diffraction experiments that such species exist in the Pu(IV)-cit system (data not shown). Additionally, the presence of a strong absorbance band at 498 nm in this work (and the lack thereof for the Pu(IV)-acetate hexamer) likely suggests an alternate Pu(IV)-cit species.

Pu(IV) solubility modeling in the presence of citrate indicates that Pu(IV) hydrolysis and subsequent precipitation will outcompete citrate complexation under neutral to alkaline conditions (Figures 5c,d and S2). Models utilizing stability constants from Metivier and Guillaumont[10] were not used due to their apparent underestimation of Pu(IV) solubility in the presence of citrate compared to our experimental observations. It is therefore plausible that Pu(IV)−OH-cit species are not stable or are not necessary to describe the Pu(IV)-cit system and that the current Pu(IV)-cit speciation regime, with constants originally published by Nebel,[8,9] adequately describes Pu(IV) solubility in the presence of citrate.

3.4. Pu(III) Oxidation in the Presence of Citrate. *3.4.1. Oxidation State Analysis of the Pu(III) System.* Similar trends in the oxidation of Pu(III) to Pu(IV) were observed at each pH_m (Figure 8). The first four time points were characterized by a slightly slower rate of Pu(III) oxidation than subsequent time points. At pH_m < 3, Pu(III) was slightly more stable in the absence of citrate (Figure S7), possibly owing to the narrower stability field of Pu(IV) in that pH region,[61] and to the thermodynamic favorability of Pu(IV)-citrate complexes. Under circumneutral conditions, citrate demonstrated a slight stabilizing effect on Pu(III), where plutonium oxidized or precipitated from solution more quickly in the absence of citrate. A pH-dependent return of Pu(III) was observed for citrate-bearing reactors (along with a decrease in pe values (Figure S2)), where, after 158 days, increasing concentrations of Pu(III) were observed with decreasing pH (along with small fractions of Pu(V) present in the pH_m 2.92 reactor). The most plausible explanation for this is the disproportionation of Pu(IV). While Pu(IV) disproportionation has an inverse fourth-order dependence on pH, the lower stabilities of Pu(III) and Pu(V) under neutral to alkaline, "redox-neutral" conditions (pe + pH = 13.8),[70] would help to explain the relative oxidation state distributions at those latter sampling points.

Equilibrium of aqueous Pu(III) and Pu(IV) with colloidal Pu(IV) species in reactors with excess citrate is also possible, as evidenced by the removal of approximately 20% of plutonium via filtration with 3 kDa filters from circumneutral reactors (Figure 8). The phase removed by filtration is expected to be Pu(IV) based on the relative predominance of aqueous Pu(IV) obtained from solvent extraction (suggesting equilibrium with a Pu(IV) solid and/or colloidal phase) and observed pe values (Figure S2). A constant $\log[Pu(IV)_{coll}] = -8.3 \pm 1.0$ is expected for Pu(IV) colloids under neutral to alkaline conditions.[72] However, the effect of organic ligands on the Pu(IV) colloid formation is not well understood. While Hummel et al.[3] considered colloids with respect to how they might influence thermodynamic data, they did not discuss colloidal characteristics or factors (such as ligating molecules) that could affect their formation.

3.4.2. Pu(III) Kinetic Modeling. Reaction rates for Pu(III) oxidation in the presence of citrate were treated as pseudo-first-order reactions. The difference in Pu(III) oxidation rates before and after approximately 43 days (Figure 9) is attributed to the generation of oxidizing radiolysis products, namely, H_2O_2, which has a long enough half-life in solution to interact with plutonium.[73] Concentrations of radicals generated from the α radiolysis of water by ^{239}Pu as a function of time were

https://doi.org/10.1021/acs.est.4c02803
Environ. Sci. Technol. 2024, 58, 15766−15778

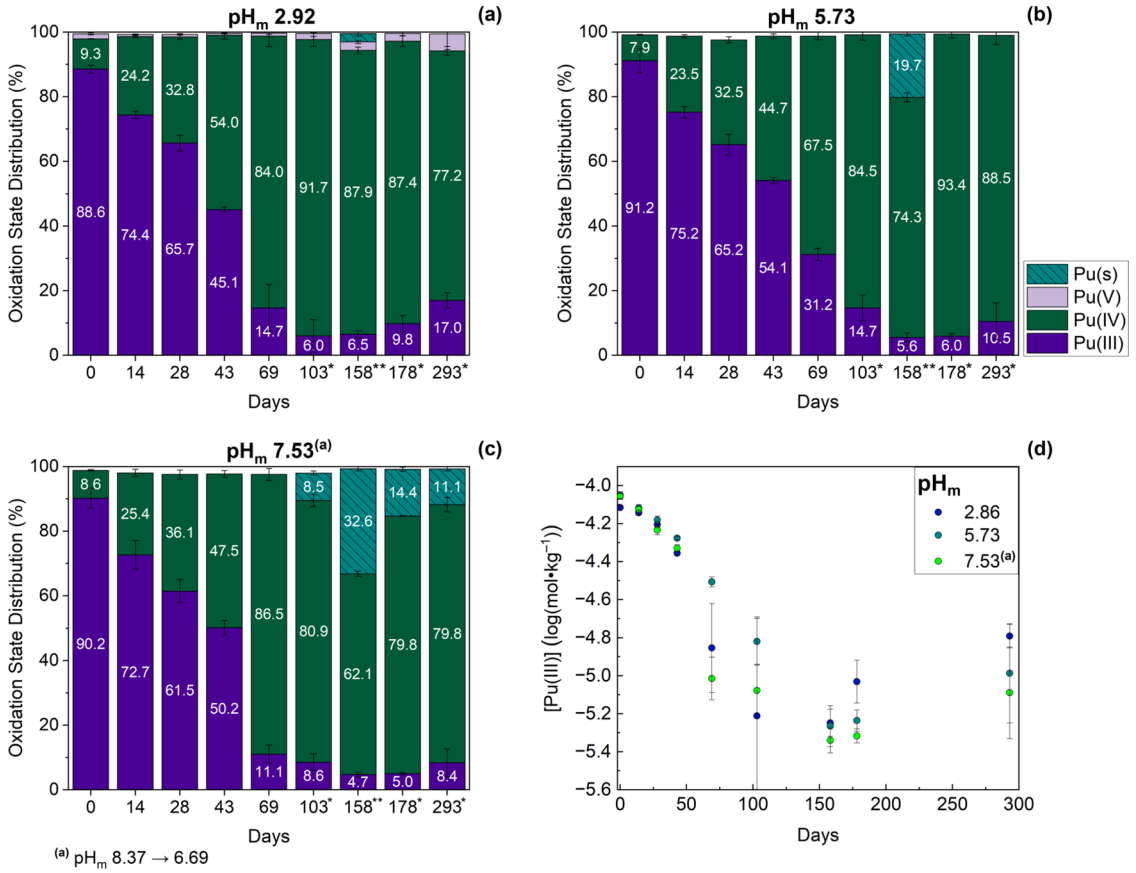

Figure 8. Oxidation state distributions for the Pu(III)-citrate system obtained from solvent extraction using 0.5 M HDEHP and 0.025 M PMBP as extractants (a–c) and $\log_{10}$ of the molality of Pu(III) in each reactor throughout the experimental period (d). Single asterisks indicate filtration through 10 kDa filters (pore size ≈2.5 nm), and double asterisks indicate filtration through 3 kDa filters (pore size ≈1.5 nm),[71] with centrifuge speeds of 14,000 rpm for 10 min in both cases. $[Pu]_T = 0.093 \pm 0.001$ mM, $[cit]_T = 1.00 \pm 0.02$ mM, and $I = 0.1$ M NaCl. Pu(s) is used to account for precipitated Pu of any oxidation state.

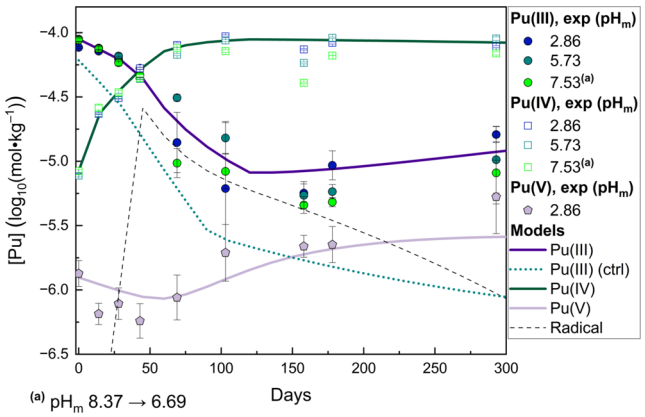

Figure 9. Kinetic model of the Pu(III)-citrate system. The deviation of experimental data from modeled Pu(III) and Pu(IV) concentrations at the 158-day time point is from the use of 3 kDa filters.

calculated using a linear equation relating α particle energy to the G value (number of molecules per 100 eV) for each radical species,[74] combined with the half-lives of ^{239}Pu ($t_{1/2}$ = 24,100 years) and ^{240}Pu ($t_{1/2}$ = 6,552 years) (Table S5). An emission energy of 5.1514 MeV was obtained by taking the weighted average of all possible ^{239}Pu decay modes.[75] The decay energies from other Pu isotopes and radical degradation were not included in the model. First-order rate constants for radical generation were determined from the calculated radical concentrations, resulting in minor variation among rate constants calculated for differing lengths of time (Table S6); we found that rate constants determined within 50–150 days best fit our experimental observations of Pu(III) oxidation.

Though H_2O_2 is known to persist in solution, Pu(III) could be oxidized by other radiolysis products, such as oxidizing chloride species (e.g., ClO^-, ClO_2^-) produced from their reaction with OH radicals,[76] which have been shown to oxidize ferrous iron.[77] While oxidizing chloride species, which were not included in these calculations, may contribute to the total concentration of radicals, it is also possible that thermodynamics contributes to the oxidation of Pu(III), given the lack of Pu(III) stability under redox-neutral conditions.[61] For example, the redox transformation $Pu^{III}(citH)_2^{3-} \rightleftharpoons Pu^{IV}(citH)_2^{2-} + e^-$ has an $E° = 0.208$ V (using Pu(IV)-cit stability constants from Nebel[8,9]). The greater thermodynamic stability of Pu(IV)-cit complexes ($\log \beta°(Pu^{IV}(citH)_2^{2-}) = 35.1$ versus $\log \beta°(Pu^{III}(citH)_2^{3-}) = 13.9$ [Am analog])[3] explains the outsized proportion of Pu(IV) to Pu(III) in solution, and may support our observations of an increased rate of Pu(III) oxidation with time. The small shift in solution pe required to change from Pu(IV) to Pu(III) complexes along with the contribution of Pu(III) species observed in our reactors throughout the experimental period demonstrates the potential significance of Pu(III) species in the WIPP and other repositories.

https://doi.org/10.1021/acs.est.4c02803
Environ. Sci. Technol. 2024, 58, 15766–15778

Table 3. Rate Constants for the Pu(III)-Citrate System (pH_m 2.8−8.4) and Pu(III) in the Absence of Citrate (pH_m 5.5) as a Function of Ligand-to-Metal Ratio (L/M)[a]

reaction	rate constant (log_{10}), k L/M = 10	rate constant (log_{10}), k L/M = 0	k units
$Pu(III) \rightarrow Pu(IV)$	−6.84	−6.51	s^{-1}
$Pu(III) + radical \rightarrow Pu(IV)$	−1.89	−1.89	$M^{-1}\ s^{-1}$
$Pu(V) \rightarrow Pu(IV)$	−7.00	−6.23	s^{-1}
oxidizing radical generation	−5.53	−5.53	s^{-1}
$3Pu(V) + 4H^+ \rightarrow Pu(III) + 2Pu(VI) + 2H_2O$	0.18	−0.68	$M^{-6}\ s^{-1}$
$3Pu(IV) + 2H_2O \rightarrow 2Pu(III) + Pu(VI) + 4H^+$	−0.35	−1.35	$M^{-4}\ s^{-1}$

[a]Uncertainty for rate constants is ±0.01 log_{10} units (2σ).

A rate constant of $log_{10}(k) = -1.89$ was assigned to the radical-mediated oxidation of Pu(III) to Pu(IV) (Table 3). While it is likely that this reaction would happen much faster,[73,77] PHREEQC will fail with reaction rates that are too disparate. Thus, some uncertainty exists regarding both the radical species and the rates of Pu(III) oxidation by radicals (i.e., the generation of oxidizing radicals may be slower and the interaction between Pu(III) and the radical may be faster than what is included in our model).

In the presence of excess citrate under circumneutral conditions, the greater stability of Pu(III) and the lower stability of Pu(V) are reflected by the rate constants in Table 3 and supported by our observations from the Pu(VI)-citrate system. The precipitation of plutonium, as seen in the Pu(III) controls (Figure S7), may have inhibited the rate of oxidation by trapping α particles within the solid phase (thereby limiting the production of radiolysis products). Thus, a faster rate of oxidation may occur in the absence of precipitation for the system without citrate, further supporting our observations of faster Pu(III) oxidation in the absence of citrate. Nonetheless, the presence of Pu(III) in the Pu-cit reactors throughout the 293-day sampling period is consistent with previous observations of Pu(III) stabilization in the presence of organic ligands[27,28] and warrants further attention with respect to other repository-relevant organic ligands that may exhibit similar effects.

3.5. Citrate-Mediated Reduction of Plutonium. The reaction rates determined in this work highlight an apparent reducing capacity of citrate toward plutonium, where more oxidized forms of plutonium exhibit faster rates of reduction in the presence of citrate than without. Likewise, aqueous Pu(III) exhibits a slightly greater stability with citrate present, especially under circumneutral to alkaline conditions. The effect of radiation on both the oxidation of organic molecules and the radiolytic or photolytic ligand-mediated reduction of metals are processes that are well understood.[78−87] Though microbial activity has been shown to influence plutonium oxidation state,[88,89] and may reduce Pu or metabolize citrate in Pu-cit complexes,[5,22] an 81-day investigation of citrate stability in the absence of plutonium under oxic laboratory conditions did not reveal any evidence for microbial citrate degradation (results not shown).

We hypothesize that citrate undergoes oxidative decarboxylation facilitated by α radiolysis from ^{239}Pu in solution. Specifically, we know that OH radicals preferentially attack the α-carbon position of amino acids and other nitrogen-bearing compounds.[78,79] A similar mechanism of ligand degradation is reported for edta in the Co(II/III)-edta system,[82,83] where electron transfer occurs from the oxidative breakdown of edta, resulting in reactive edta radicals and subsequent reduction of the metal center. A similar mechanism could be applied to the Pu-cit system, where the methylene groups serve as the α-carbon sites. After interaction with an oxidizing radical, intramolecular electron transfer is expected to occur between citrate and Pu. The primary citrate degradation product in the presence of γ irradiation was found to be malonic acid.[7] The self-irradiation of weapons-grade Pu is almost 3 times stronger than that of the ^{60}Co source used in the aforementioned studies.[90] Understanding such processes that may be facilitated by radiolytic effects is especially pertinent to the WIPP, where the current plutonium inventory could more than triple before the facility's closure.[2]

3.6. Environmental Implications. It is clear from the present work, based on speciation determinations from pH_m 2.5 to 10.9 and accompanying oxidation state distributions with time, that citrate enhances the reduction of plutonium, especially higher-valent plutonium under the neutral to alkaline conditions relevant to the WIPP. This interaction may be facilitated by the presence of oxidizing radiolysis species, which have previously been shown to result in simultaneous ligand degradation and metal reduction.[78−84]

Pu(III) persisted in solution for longer under circumneutral conditions with citrate present. We have shown that, due to plutonium disproportionation reactions, the suspected reduction by citrate, and the minor change in solution pe required to transform $Pu^{(III)}(citH)_2^{3-}$ to $Pu^{(IV)}(citH)_2^{2-}$, some degree of Pu(III) may persist in equilibrium with Pu(IV) throughout the life of the repository, in agreement with past observations.[27,28] The actual proportion of Pu(III) may be greater than predicted in the present work when considering the more strongly reducing conditions of the WIPP, the presence of reducing iron species, additional organic ligand types, higher radioactivity, etc. Therefore, more work is needed to determine the extent to which WIPP-relevant organic ligands will stabilize plutonium in its trivalent state.

We have shown that minimal Pu(IV)-cit complexation takes place at $pH_m > 8$, implying that citrate may have little influence over Pu(IV) mobility in a repository setting and further emphasizing the need to accurately predict the ratio of Pu(III/IV) in the WIPP to better determine whether citrate poses a risk of mobilizing Pu.

■ ASSOCIATED CONTENT

Supporting Information

The Supporting Information is available free of charge at https://pubs.acs.org/doi/10.1021/acs.est.4c02803.

Additional methods descriptions (pH and E_h measurements, validity of the solvent extraction technique), ion

https://doi.org/10.1021/acs.est.4c02803
Environ. Sci. Technol. 2024, 58, 15766−15778

interaction coefficients and stability constants used in equilibrium modeling, experimental Pu concentrations, peak centers, molar extinction coefficients, and deconvolution information for Pu(VI) spectra, solubility curves and Pourbaix diagrams for long-term experiments, additional kinetic models, oxidation state distributions for Pu(VI) and Pu(III) controls, Pu(III) UV−vis spectra, G values, and linear equations used in determining radical concentrations and rate constants (PDF)

AUTHOR INFORMATION

Corresponding Author

Amy E. Hixon − *Department of Civil & Environmental Engineering & Earth Sciences, University of Notre Dame, Notre Dame, Indiana 46556, United States;* orcid.org/0000-0003-4513-4574; Email: ahixon@nd.edu

Authors

Matthew B. Comins − *Department of Civil & Environmental Engineering & Earth Sciences, University of Notre Dame, Notre Dame, Indiana 46556, United States;* orcid.org/0000-0003-0863-6102

Ugras Kaplan − *Los Alamos National Laboratory, Carlsbad, New Mexico 88220, United States*

Jeremiah Beam − *Los Alamos National Laboratory, Carlsbad, New Mexico 88220, United States*

Adrianne Navarrette − *Los Alamos National Laboratory, Carlsbad, New Mexico 88220, United States*

Complete contact information is available at: https://pubs.acs.org/10.1021/acs.est.4c02803

Notes

The authors declare no competing financial interest.

ACKNOWLEDGMENTS

This research was supported, in part, by the Arthur J. Schmitt Fellowship and by an appointment to the DOE Scholars Program, sponsored by the U.S. Department of Energy, administered by the Oak Ridge Institute for Science and Education, and funded by the WIPP Project (DOE-CFBO). Lastly, the authors are grateful to Donald T. Reed and Jean-Francois Lucchini, whose insight and ideas regarding actinide repository science contributed to the methods and success of these studies.

REFERENCES

(1) Gerle, M. *Annual Transuranic Waste Inventory Report*, DOE/TRU-22-3425; U.S. Department of Energy, Carlsbad Field Office, 2022.

(2) U.S. Department of Energy. *Final Environmental Impact Statement for the Surplus Plutonium Disposition Program*, DOE/EIS-0549; U.S. Department of Energy, 2023.

(3) Hummel, W.; Anderegg, G.; Rao, L.; Puigdomènech, I.; Tochiyama, O. *Chemical Thermodynamics of Compounds and Complexes of U, Np, Pu, Am, Tc, Se, Ni and Zr with Selected Organic Ligands*; OECD Publishing, 2005; Vol. 9, p 1130.

(4) Toste, A. P.; Lechner-Fish, T. J. Chemo-Degradation of Chelating and Complexing Agents in a Simulated, Mixed Nuclear Waste. *Waste Manage.* **1993**, *13* (3), 237−244.

(5) Francis, A. J.; Dodge, C. J.; Gillow, J. B. Biotransformation of Plutonium Complexed with Citric Acid. *Radiochim. Acta* **2006**, *94* (9−11), 731−737.

(6) Toste, A. P. Degradation of Chelating and Complexing Agents in an Irradiated, Simulated Mixed Waste. *J. Radioanal. Nucl. Chem.* **1992**, *161* (2), 549−559.

(7) Toste, A. P.; Polach, K. J.; White, T. W. Degradation of citric acid in a simulated, mixed nuclear waste: Radiolytic versus chemical forces. *Waste Manage.* **1994**, *14* (1), 27−34.

(8) Nebel, D. Spektralphotometrische Untersuchung des Gleichgewichtes PuIV-Citrat in wäßriger Lösung. *Z. Phys. Chem.* **1966**, *232*, 161−175.

(9) Nebel, D. Potentiometrische Untersuchungen des Gleichgewichtes PuIV-Citrat in wäßriger Lösung. *Z. Phys. Chem.* **1966**, *232O*, 368−376.

(10) Metivier, H.; Guillaumont, R. Complexes Citriques Du Plutonium Tetravalent. *Radiochem. Radioanal. Lett.* **1972**, *10*, 239−250.

(11) Nebel, D.; Anders, G. Zur Komplexbildung und Solvatation einiger Actinide I. Untersuchungen zur Komplexbildung mit Acetat und Citrat. *Isotopenpraxis* **1975**, *11* (4), 152−155.

(12) Svoronos, D.-R.; Boulhassa, S.; Guillaumont, R.; Guillamont, R. Citric complexes and neodymium citrate: NdCit, $3H_2O$. *J. Inorg. Nucl. Chem.* **1981**, *43*, 1541−1545.

(13) Raymond, D. P.; Duffield, J. R.; Williams, D. R. Complexation of Plutonium and Thorium in Aqueous Environments. *Inorg. Chim. Acta* **1987**, *140*, 309−313.

(14) Poczynajło, A. Potentiometric Determination of Pu(III) Complexes Formed by Citric Acid, EDTA, DHTP and DTPP. *J. Radioanal. Nucl. Chem.* **1989**, *134* (1), 97−108.

(15) Kantar, C.; Honeyman, B. D. Plutonium (IV) Complexation with Citric and Alginic Acids at Low Pu_T Concentrations. *Radiochim. Acta* **2005**, *93* (12), 757−766.

(16) Bonin, L.; Cote, G.; Moisy, P. Speciation of An(IV) (Pu, Np, U and Th) in Citrate Media. *Radiochim. Acta* **2008**, *96* (3), 145−152.

(17) Thakur, P.; Pathak, P. N.; Choppin, G. R. Complexation Thermodynamics and the Formation of the Binary and the Ternary Complexes of Tetravalent Plutonium with Carboxylate and Aminocarboxylate Ligands in Aqueous Solution of High Ionic Strength. *Inorg. Chim. Acta* **2009**, *362* (1), 179−184.

(18) Heller, A.; Barkleit, A.; Foerstendorf, H.; Tsushima, S.; Heim, K.; Bernhard, G. Curium(III) Citrate Speciation in Biological Systems: A Europium(III) Assisted Spectroscopic and Quantum Chemical Study. *Dalton Trans.* **2012**, *41* (45), 13969.

(19) Brown, M. A.; Kropf, A. J.; Paulenova, A.; Gelis, A. V. Aqueous Complexation of Citrate with Neodymium(III) and Americium(III): A Study by Potentiometry, Absorption Spectrophotometry, Microcalorimetry, and XAFS. *Dalton Trans.* **2014**, *43* (17), 6446.

(20) Aoyagi, N.; Palladino, G.; Nagasaki, S.; Kimura, T. Optical Properties of Trinuclear Citrate Complexes Containing 4f and 5f Block Metals. *Bull. Chem. Soc. Jpn.* **2018**, *91* (6), 882−890.

(21) Tamain, C.; Bonato, L.; Aupiais, J.; Dumas, T.; Guillaumont, D.; Barkleit, A.; Berthon, C.; Solari, P. L.; Ikeda-Ohno, A.; Guilbaud, P.; Moisy, P. Role of the Hydroxo Group in the Coordination of Citric Acid to Trivalent Americium. *Eur. J. Inorg. Chem.* **2020**, *2020* (14), 1331−1344.

(22) Francis, A. J.; Dodge, C. J.; Ohnuki, T. Microbial Transformations of Plutonium. *J. Nucl. Radiochem. Sci.* **2007**, *8* (2), 121−126.

(23) Moutte, A.; Guillaumont, R. Complexes Citriques d'actinium et de Curium. *Rev. Chim. Miner.* **1969**, *6* (3), 603−610.

(24) Bouhlassa, S.; Guillamont, R. Conditions de Formation, Caracteristiques Cristallographiques et Spectroscopiques de Citrates de Neodyme. *Bull. Soc. Chim. Fr.* **1984**, 12−18.

(25) Eberle, S. H.; Moattar, F. Die Komplexe Des Am(III) Mit Zitronensäure. *Inorg. Nucl. Chem. Lett.* **1972**, *8* (3), 265−272.

(26) Reed, D. T.; Wygmans, D. G.; Aase, S. B.; Banaszak, J. E. Reduction of Np(VI) and Pu(VI) by Organic Chelating Agents. *Radiochim. Acta* **1998**, *82*, 109−114.

(27) Al Mahamid, I.; Becraft, K. A.; Hakem, N. L.; Gatti, R. C.; Nitsche, H. Stability of Various Plutonium Valence States in the

Presence of NTA and EDTA. *Radiochim. Acta* **1996**, *74* (s1), 129−134.
(28) Rai, D.; Moore, D. A.; Rosso, K. M.; Felmy, A. R.; Bolton, H. Environmental Mobility of Pu(IV) in the Presence of Ethylenediaminetetraacetic Acid: Myth or Reality? *J. Solution Chem.* **2008**, *37* (7), 957−986.
(29) Schramke, J. A.; Santillan, E. F. U.; Peake, R. T. Plutonium Oxidation States in the Waste Isolation Pilot Plant Repository. *Appl. Geochem.* **2020**, *116*, No. 104561.
(30) Paiva, A. P.; Malik, P. Recent Advances on the Chemistry of Solvent Extraction Applied to the Reprocessing of Spent Nuclear Fuels and Radioactive Wastes. *J. Radioanal. Nucl. Chem.* **2004**, *261* (2), 485−496.
(31) Einkauf, J. D.; Burns, J. D. Solid State Characterization of Oxidized Actinides Co-Crystallized with Uranyl Nitrate Hexahydrate. *Dalton Trans.* **2020**, *49* (3), 608−612.
(32) Lucchini, J. F.; Borkowski, M.; Khaing, H.; Richmann, M. K.; Swanson, J. S.; Simmons, K.; Reed, D. T. *WIPP Actinide-Relevant Brine Chemistry*, LCO-ACP-15. LA-UR 13-20620; Los Alamos National Laboratory: Carlsbad, NM, 2013.
(33) Lloyd, M. H.; Haire, R. G. The Chemistry of Plutonium in Sol-Gel Processes. *Radiochim. Acta* **1978**, *25*, 139−148.
(34) Virot, M.; Dumas, T.; Cot-Auriol, M.; Moisy, P.; Nikitenko, S. I. Synthesis and Multi-Scale Properties of PuO_2 Nanoparticles: Recent Advances and Open Questions. *Nanoscale Adv.* **2022**, *4* (23), 4938−4971.
(35) Nitsche, H.; Lee, S. C.; Gatti, R. C. Determination of Plutonium Oxidation States at Trace Levels Pertinent to Nuclear Waste Disposal. *J. Radioanal. Nucl. Chem.* **1988**, *124* (1), 171−185.
(36) Neu, M. P.; Hoffman, D. C.; et al. Comparison of Chemical Extractions and Laser Photoacoustic Spectroscopy for the Determination of Plutonium Species in Near-Neutral Carbonate Solutions. *Radiochim. Acta* **1994**, *66*−*67*, 251−258.
(37) Hixon, A. E.; Arai, Y.; Powell, B. A. Examination of the Effect of Alpha Radiolysis on Plutonium(V) Sorption to Quartz Using Multiple Plutonium Isotopes. *J. Colloid Interface Sci.* **2013**, *403*, 105−112.
(38) Minns, J. L.; Wenzel, A. W.; Hedrick, C. E.; Pietri, C. E. *Adjustment of Plutonium Oxidation State by Ferrous and Dichromate Ion Treatment − A Preliminary Study*; NBL-265; New Brunswick Laboratory, 1972; pp 90−93.
(39) Tasi, A.; Gaona, X.; Fellhauer, D.; Böttle, M.; Rothe, J.; Dardenne, K.; Schild, D.; Grivé, M.; Colàs, E.; Bruno, J.; Källström, K.; Altmaier, M.; Geckeis, H. Redox Behavior and Solubility of Plutonium under Alkaline, Reducing Conditions. *Radiochim. Acta* **2018**, *106* (4), 259−279.
(40) Nelson, D. M.; Lovett, M. B. Oxidation State of Plutonium in the Irish Sea. *Nature* **1978**, *276*, 599−601.
(41) Kobashi, A.; Choppin, G. R.; Morse, J. W. A Study of Techniques for Separating Plutonium in Different Oxidation States. *Radiochim. Acta* **1988**, *43* (4), 211−215.
(42) Gehmecker, H.; Trautmann, N.; Herrmann, G. Extraction of Pu^{3+}, Pu^{4+} and PuO_2^{2+} from Various Mineral Acid Solutions by Tri-n-Butylphosphate and Di-(2-Ethylhexyl)-Orthophosphoric Acid. *Radiochim. Acta* **1986**, *40*, 11−15.
(43) Manchanda, V. K.; Mohapatra, P. K. 1-Phenyl-3-Methyl-4-Benzoyl-Pyrazolone-5: A Promising Extractant for Plutonium. *Sep. Sci. Technol.* **1994**, *29* (8), 1073−1086.
(44) Reilly, S. D.; Neu, M. P. Pu(VI) Hydrolysis: Further Evidence for a Dimeric Plutonyl Hydroxide and Contrasts with U(VI) Chemistry. *Inorg. Chem.* **2006**, *45* (4), 1839−1846.
(45) Rao, L.; Tian, G.; Di Bernardo, P.; Zanonato, P. Hydrolysis of Plutonium(VI) at Variable Temperatures (283−343 K). *Chem.—Eur. J.* **2011**, *17* (39), 10985−10993.
(46) Pashalidis, I.; Kim, J. I.; Ashida, T.; Grenthe, I. Spectroscopic Study of the Hydrolysis of PuO_2^{2+} in Aqueous Solution. *Radiochim. Acta* **1995**, *68* (2), 99−104.
(47) Cho, H.-R.; Jung, E. C.; Park, K. K.; Kim, W. H.; Song, K.; Yun, J.-I. Spectroscopic Study on the Mononuclear Hydrolysis Species of Pu(VI) under Oxidation Conditions. *Radiochim. Acta* **2010**, *98* (12), 765−770.
(48) Kretzschmar, J.; Tsushima, S.; Lucks, C.; Jäckel, E.; Meyer, R.; Steudtner, R.; Müller, K.; Rossberg, A.; Schmeide, K.; Brendler, V. Dimeric and Trimeric Uranyl(VI)−Citrate Complexes in Aqueous Solution. *Inorg. Chem.* **2021**, *60*, 7998−8010.
(49) Silva, A. M. N.; Kong, X.; Hider, R. C. Determination of the pKa Value of the Hydroxyl Group in the α-Hydroxycarboxylates Citrate, Malate and Lactate by 13C NMR: Implications for Metal Coordination in Biological Systems. *BioMetals* **2009**, *22* (5), 771−778.
(50) Strouse, J. Carbon-13 NMR Studies of Ferrous Citrates in Acidic and Alkaline Solutions. Implications Concerning the Active Site of Aconitase. *J. Am. Chem. Soc.* **1977**, *99* (2), 572−580.
(51) Hedwig, G. R.; Liddle, J. R.; Reeves, R. D. Complex Formation of Nickel(II) Ions with Citric Acid in Aqueous Solution: A Potentiometric and Spectroscopic Study. *Aust. J. Chem.* **1980**, *33*, 1685−1693.
(52) Öhman, L.-O. Equilibrium and Structural Studies of Silicon(IV) and Aluminum(III) in Aqueous Solution. 17. Stable and Metastable Complexes in the System H^+−Al^{3+}−Citric Acid. *Inorg. Chem.* **1988**, *27* (15), 2565−2570.
(53) Baker, E. N.; Baker, H. M.; Anderson, B. F.; Reeves, R. D. Chelation of Nickel(II) by Citrate. The Crystal Structure of a Nickel-Citrate Complex, $K_2[Ni(C_6H_5O_7)(H_2O)_2]_2 \bullet 4H_2O$. *Inorg. Chim. Acta* **1983**, *78*, 281−285.
(54) Chunbo, Y.; Juzheng, L.; Daqing, Z.; Yijie, W.; Jiazuan, N. Lanthanide-Induced Shift and Relaxation Rate Studies of the Aqueous Complexation of Citrate. *Polyhedron* **1995**, *14* (23−24), 3579−3583.
(55) Kieboom, A. P. G.; Vijverberg, C. A. M.; Peters, J. A.; Van Bekkum, H. Complexation of Acetate, Glycolate, Lactate, Malate and Citrate Anions with Lanthanide(III) Cations in Aqueous Solution as Studied by NMR Spectroscopy. *Recl. Trav. Chim. Pays-Bas* **1977**, *96* (12), 315−316.
(56) Silva, A. M. N.; Kong, X.; Parkin, M. C.; Cammack, R.; Hider, R. C. Iron(III) Citrate Speciation in Aqueous Solution. *Dalton Trans.* **2009**, No. 40, 8616.
(57) Motekaitis, R. J.; Martell, A. E. Complexes of Aluminum(III) with Hydroxy Carboxylic Acids. *Inorg. Chem.* **1984**, *23* (1), 18−23.
(58) Clausén, M.; Öhman, L.-O.; Persson, P. Spectroscopic Studies of Aqueous Gallium(III) and Aluminum(III) Citrate Complexes. *J. Inorg. Biochem.* **2005**, *99* (3), 716−726.
(59) Cho, H.-R.; Jung, E. C.; Park, K. K.; Song, K.; Yun, J.-I. Effect of Reduction on the Stability of Pu(VI) Hydrolysis Species. *Radiochim. Acta* **2010**, *98* (9−11), 555−561.
(60) Hixon, A. E.; Powell, B. A. Plutonium Environmental Chemistry: Mechanisms for the Surface-Mediated Reduction of Pu(V/VI). *Environ. Sci.: Processes Impacts* **2018**, *20* (10), 1306−1322.
(61) Altmaier, M.; Xavier, G.; Fellhauer, D.; Clark, D. L.; Runde, W. H.; Hobart, D. E. Aqueous Solution and Coordination Chemistry of Plutonium. In *Plutonium Handbook*; Clark, D. L.; Geeson, D. A.; Hanrahan, R. J., Eds.; 2019; Vol. *3*, pp 1543−1726.
(62) Connick, R. E. Mechanism of the Disproportionation of Plutonium (V). *J. Am. Chem. Soc.* **1949**, *71* (5), 1528−1533.
(63) Pilling, M. J.; Seakins, P. W. *Reaction Kinetics*; Oxford University Press: New York, 1995.
(64) Ohyoshi, E.; Ohyoshi, A. A study of complexes with a polybasic acid. *J. Inorg. Nucl. Chem.* **1971**, *33*, 4265−4273.
(65) Ohyoshi, A.; Ohyoshi, E.; Ono, H.; Yamakawa, S. A study of citrate complexes of several lanthanides. *J. Inorg. Nucl. Chem.* **1972**, *34*, 1955−1960.
(66) Bouhlassa, S.; Guillaumont, R. Complexes citriques et citrates d'américium. *J. Less-Common Met.* **1984**, *99*, 157−171.
(67) Fedosseev, A. M.; Grigoriev, M. S.; Budantseva, N. A.; Guillaumont, D.; Le Naour, C.; Simoni, É.; Den Auwer, C.; Moisy, P. Americium(III) Coordination Chemistry: An Unexplored Diversity of Structure and Bonding. *C. R. Chim.* **2010**, *13* (6−7), 839−848.
(68) Tamain, C.; Dumas, T.; Hennig, C.; Guilbaud, P. Coordination of Tetravalent Actinides (An = Th^{IV}, U^{IV}, Np^{IV}, Pu^{IV}) with DOTA:

https://doi.org/10.1021/acs.est.4c02803
Environ. Sci. Technol. 2024, 58, 15766−15778

From Dimers to Hexamers. *Chem.—Eur. J.* **2017**, *23* (28), 6864−6875.
(69) Chupin, G.; Tamain, C.; Dumas, T.; Solari, P. L.; Moisy, P.; Guillaumont, D. Characterization of a Hexanuclear Plutonium(IV) Nanostructure in an Acetate Solution via Visible−Near Infrared Absorption Spectroscopy, Extended X-Ray Absorption Fine Structure Spectroscopy, and Density Functional Theory. *Inorg. Chem.* **2022**, *61* (12), 4806−4817.
(70) Neck, V.; Altmaier, M.; Fanghänel, T. Solubility of Plutonium Hydroxides/Hydrous Oxides under Reducing Conditions and in the Presence of Oxygen. *C. R. Chim.* **2007**, *10*, 959−977.
(71) Schäfer, A. I.; Mauch, R.; Waite, T. D.; Fane, A. G. Charge Effects in the Fractionation of Natural Organics Using Ultrafiltration. *Environ. Sci. Technol.* **2002**, *36* (12), 2572−2580.
(72) Neck, V.; Altmaier, M.; Seibert, A.; Yun, J. I.; Marquardt, C. M.; Fanghänel, T. Solubility and Redox Reactions of Pu(IV) Hydrous Oxide: Evidence for the Formation of PuO_{2+x}(s, Hyd). *Radiochim. Acta* **2007**, *95* (4), 193−207.
(73) Pastina, B.; LaVerne, J. A. Effect of Molecular Hydrogen on Hydrogen Peroxide in Water Radiolysis. *J. Phys. Chem. A* **2001**, *105* (40), 9316−9322.
(74) Turner, J. E. *Atoms, Radiation, and Radiation Protection*; Wiley-VCH: Germany, 2007.
(75) International Atomic Energy Agency. Live Chart of Nuclides, 2023. https://www-nds.iaea.org/relnsd/vcharthtml/VChartHTML.html.
(76) Paviet-Hartmann, P.; Dziewinski, J.; Hartmann, T.; Marczak, S.; Lu, N.; Walthall, M.; Rafalski, A.; Zagorski, Z. P. In *Spectroscopic Investigation of the Formation of Radiolysis By-Products By 13/9 MeV Linear Accelerator of Electrons (LAE) in Salt Solutions*, Conference: Waste Management 2002 Symposium, Tucson, AZ; US Department of Energy, 2002.
(77) Jayson, G. G.; Parsons, B. J.; Swallow, A. J. The Mechanism of the Fricke Dosimeter. *Int. J. Radiat. Phys. Chem.* **1975**, *7* (2−3), 363−370.
(78) Garrison, W. M.; Jayko, M. E.; Bennett, W. Radiation-Induced Oxidation of Protein in Aqueous Solution. *Radiat. Res.* **1962**, *16* (4), 483−502.
(79) Garrison, W. M. Actions of Ionizing Radiations on Nitrogen Compounds in Aqueous Media. *Radiat. Res., Suppl.* **1964**, *4*, 158−174.
(80) Sugimori, A.; Tsuchihashi, G. Effect of Metal Ions on the Radiation-Induced Decarboxylation of Aqueous Benzoic and Salicylic Acid Solutions. *Bull. Chem. Soc. Jpn.* **1960**, *33* (5), 713−714.
(81) Sugimori, A. The Radiolysis of Crystalline Oxalato Metal Complexes. The Effects of Coordinating Metal Ions on the Radiolysis of Oxalate. *Bull. Chem. Soc. Jpn.* **1966**, *39* (12), 2583−2588.
(82) Matsuura, N.; Shinohara, N.; Nishikawa, M.; Takizawa, M. Radiolysis of Co^{III}-EDTA in Aqueous Solution; the Yields of Hydrogen and Hydrogen Peroxide in 0.8 N Sulfuric Acid. *Bull. Chem. Soc. Jpn.* **1967**, *40* (9), 2042−2047.
(83) Matsuura, N.; Shinohara, N.; Nishikawa, M.; Takizawa, M. Radiolysis of Co^{III}-EDTA in Aqueous Solution; The Effect of pH. *Bull. Chem. Soc. Jpn.* **1968**, *41* (6), 1284−1288.
(84) Buchanan, D. N. E. Mössbauer spectroscopy of radiolytic and photolytic effects on ferric citrate. *J. Inorg. Nucl. Chem.* **1970**, *32*, 3531−3533.
(85) Dodge, C. J.; Francis, A. J. Photodegradation of Uranium-Citrate Complex with Uranium Recovery. *Environ. Sci. Technol.* **1994**, *28* (7), 1300−1306.
(86) Zuo, Y.; Hoigne, J. Formation of Hydrogen Peroxide and Depletion of Oxalic Acid in Atmospheric Water by Photolysis of Iron(III)-Oxalato Complexes. *Environ. Sci. Technol.* **1992**, *26* (5), 1014−1022.
(87) Frahn, J. L. The photochemical decomposition of the citrate-ferric iron comples: A study of the reaction products by paper ionophoresis. *Aust. J. Chem.* **1958**, *11*, 399−405.
(88) Neu, M. P.; Icopini, G. A.; Boukhalfa, H. Plutonium Speciation Affected by Environmental Bacteria. *Radiochim. Acta* **2005**, *93*, 705−714.
(89) Roh, C.; Kang, C.; Lloyd, J. R. Microbial Bioremediation Processes for Radioactive Waste. *Korean J. Chem. Eng.* **2015**, *32* (9), 1720−1726.
(90) Hastings, A. M.; Fairley, M.; Wasson, M. C.; Campisi, D.; Sarkar, A.; Emory, Z. C.; Brunson, K.; Fast, D. B.; Islamoglu, T.; Nyman, M.; Burns, P. C.; Gagliardi, L.; Farha, O. K.; Hixon, A. E.; LaVerne, J. A. Role of Metal Selection in the Radiation Stability of Isostructural M-UiO-66 Metal−Organic Frameworks. *Chem. Mater.* **2022**, *34* (18), 8403−8417.

https://doi.org/10.1021/acs.est.4c02803
Environ. Sci. Technol. 2024, 58, 15766−15778